

Electron holography technique for investigating thin ferromagnetic films

Akira Tonomura, Tsuyoshi Matsuda, Hideo Tanabe, Nobuyuki Osakabe, Junji Endo, Akira Fukuhara, Kohsei Shinagawa, and Hideo Fujiwara

Central Research Laboratory, Hitachi Ltd., Kokubunji, Tokyo 185, Japan

(Received 30 December 1981)

A method is presented here for observing micromagnetic structures in ferromagnetic specimens. Experimental apparatuses for forming electron holograms and for reconstructing optical images are described. Special attention is paid to factors limiting measurement precision. The technique is applied to thin ferromagnetic films, for the purpose of observing fine details of magnetization distribution in a contour map of the electron phase.

I. INTRODUCTION

Recently, observation of micromagnetic structures has come to play an increasingly important role in the development of high-density magnetic devices. Up to now, domain structures in thin ferromagnetic films have been investigated mainly by Lorentz electron microscopy.¹ Although Lorentz microscopy provides the highest spatial resolution among all conventional methods, electron microscopic images are always blurred because of the large defocusing required for magnetic contrast. Therefore, fine image details are sometimes smeared out. In addition, only an abrupt change in magnetization direction can be observed, in the way of intensity variation.

The newly developed technique of electron holography opens a new way around these difficulties. With this new method, the phase distribution of the electron beam transmitted through a specimen, which reflects the magnetization, is measured as an interference micrograph. Contour lines in the electron phase distribution are imaged so that they overlap the focused electron microscopic image. In the theoretical paper by Fukuhara *et al.*,² it was verified that they run parallel to the magnetic lines of force inside a specimen, when the specimen is uniformly thick and there is no stray field outside the specimen. Such interference micrographs are not available in conventional electron microscopes because there is no Mach-Zehnder-type electron interferometer. Electron holography is, at present, the only way for obtaining them.

The principle of electron holography was originally invented by Gabor^{3,4} for improving the resolution of electron microscopic images. The application of electron holography to magnetic domain structure observation was proposed by Cohen,¹ though this application has not yet been practically carried out, except for in some preliminary experiments.⁵⁻⁸ Only most recently has electron holography been put to practical use, through the use of a field emission electron mi-

croscope.⁹

The present paper describes the experimental details of an electron holography technique employed for magnetization observation. The results of observation of thin ferromagnetic films using this technique are then presented and discussed.

II. EXPERIMENTAL APPARATUS

A. Field emission electron microscope for hologram formation

Off-axis electron holograms are formed in the field emission electron microscope shown in Fig. 1. This microscope differs from a conventional one in two ways: a 125-kV field emission electron gun, and an electron biprism, are, respectively, used to provide a coherent electron beam, and a wave-front beam splitter for forming off-axis holograms.

Electrons are emitted from a cold $\langle 310 \rangle$ -oriented tungsten tip, through the application of a 3–6-kV electric potential between the tip and the first anode. Only 1% of the emitted electron current ($\sim 100 \mu\text{A}$) is passed through the first anode aperture.

The electrons are then accelerated through a three-stage acceleration tube to form a collimated beam, and are focused through a magnetic condenser lens. When the beam is focused on the specimen plane, its diameter is 300 Å and the divergence angle (2α) is typically 1×10^{-3} rad, which is determined by the condenser aperture size. Usually the electron beam is slightly defocused so as to illuminate a larger area, and a smaller divergence angle, down to $\sim 1 \times 10^{-7}$ rad, can be obtained depending on the defocusing distance.

Special care has to be taken in designing the illuminating system, so as not to cause the inherent characteristics of the beam coherence to deteriorate through incurring such disturbances as stray magnetic fields, current instabilities in alignment deflectors,

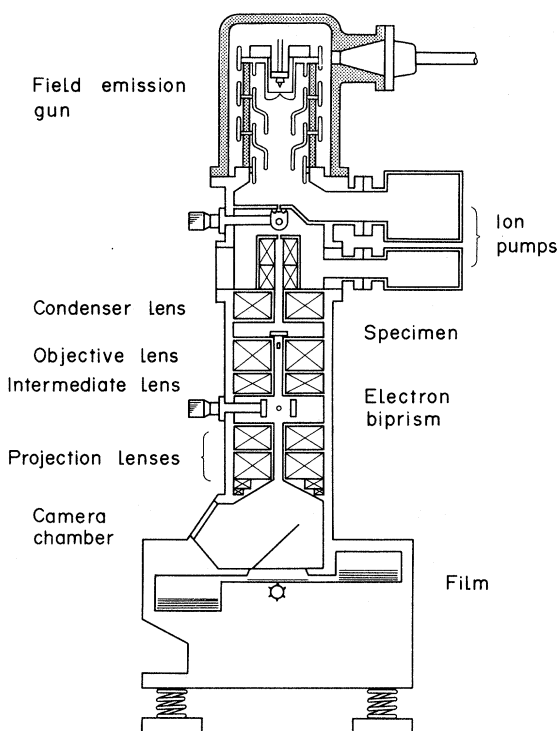


FIG. 1. Cross-sectional diagram of field emission electron microscope.

and mechanical vibration at the field emission cathode. The effects of such disturbances on the electron beam need to be suppressed to where they are $\frac{1}{100}$ times as large as for a conventional electron microscope. A third-order stigmator is also installed just below the condenser lens, in addition to the conventional second-order stigmator, in order to correct the astigmatism introduced by the electrostatic field near the first anode aperture.

The specimen position is changed to become 30 mm higher than the standard one, so as to reduce the effect of the magnetic field on the specimen. Only half a plane is used for a specimen. The other half is used for the reference beam. This limits specimen form to particle, stripe, and half-plane varieties. So far, only fine particles have been observed by this technique,¹⁰ simply because a free space for the reference beam is necessary adjacent to the specimen.

In the present experiment, thin ferromagnetic films were observed in marginal regions of half-plane specimens. The beam transmitted through a specimen, and the reference beam avoiding the specimen, are caused to overlap by an electron biprism,¹¹ so as to form an interference pattern. In actuality, the specimen is first magnified, and then the interference pattern is formed by a biprism situated under the objective or intermediate lens, whose position is select-

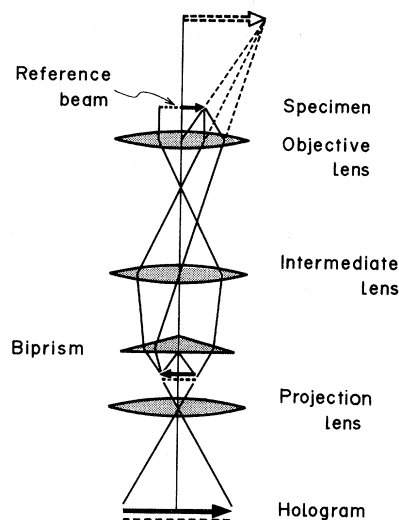


FIG. 2. Schematic diagram of electron-hologram formation.

ed depending on hologram conditions. A typical electron-optical arrangement for hologram formation is shown in Fig. 2, when the biprism is located between the intermediate and projector lenses. The interference pattern is then further magnified, and is recorded on standard electron microscopic film as a hologram. Exposure time is 5 ~ 30 sec.

A hologram is usually $5 \sim 10 \times 5 \sim 70 \text{ mm}^2$ in size, and is made up of 200 ~ 500 high-contrast biprism fringes. A larger number of fringes are desirable, since carrier spacing determines the resolution limit of the reconstructed image. The maximum number of fringes that can be recorded is mainly determined by the spatial coherence of the electron beam. It, however, also depends on such experimental conditions as specimen thickness and hologram magnification.

B. Optical system for image reconstruction

An electron hologram is placed in an optical reconstruction system for interference microscopy,¹² as shown in Fig. 3. A collimated laser beam from a He-Ne laser ($\lambda = 6328 \text{ \AA}$) is split into two beams traveling in different directions, by a Mach-Zehnder interferometer. These two beams, *A* and *B*, illuminate the hologram and produce two sets of a reconstructed image and its conjugate, whose phase distributions are opposite in sign. An interference image is observed when only the reconstructed image of beam *A*, and the transmitted beam of beam *B*, or vice versa, pass through a slit.

A contour map of the phase distribution in the electron microscopic image is obtained when the in-

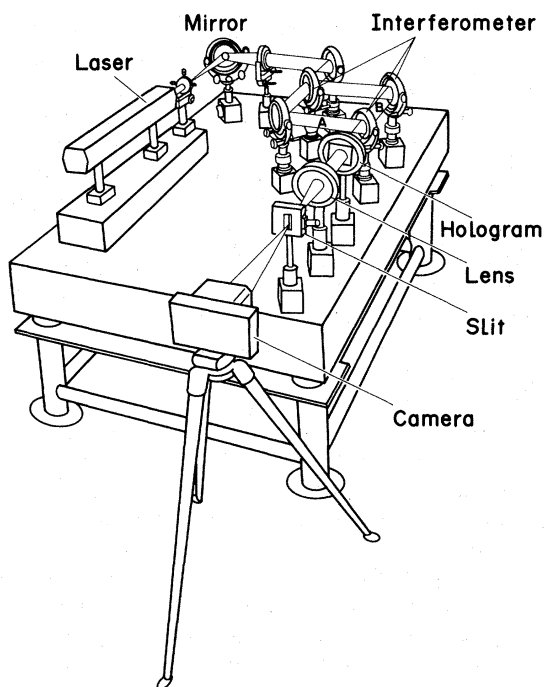


FIG. 3. Optical reconstruction system for interference microscopy.

terferometer is adjusted so that the interfering two beams may travel in the same direction. Mirrors and half-mirrors used in the Mach-Zehnder interferometer are manufactured so as to be flat enough to produce parallel interference fringes, with an accuracy of $\frac{1}{10}\lambda$, over the image field of view. Contour mapping conditions are ascertained by observing the even background, rather than through a reference system of regular fringes in the free-specimen region of an interference image.

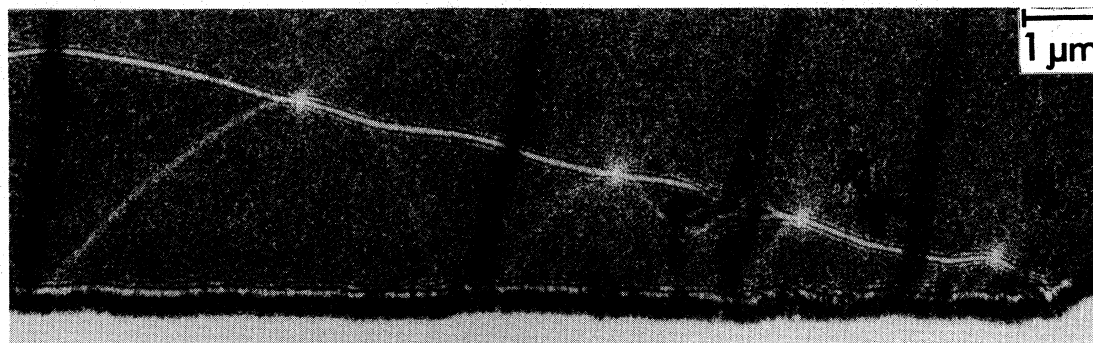
This reconstruction system can also be used for phase-amplified interference microscopy,¹³ by merely changing the selection of the two interfering beams.

III. EXPERIMENTAL RESULTS

The electron holography technique was applied for thin ferromagnetic films, using the apparatus described in Sec. II.

The principle of magnetization measurement is described in detail in Ref. 2, so only its outline will be given here.

The phase difference, $\Delta\Phi$, of the transmitted electron beam between two points in the specimen plane, is given by $(e/\hbar) \int \vec{B} \cdot d\vec{S}$. Here the integral is per-



(a) Lorentz micrograph



(b) Interference micrograph

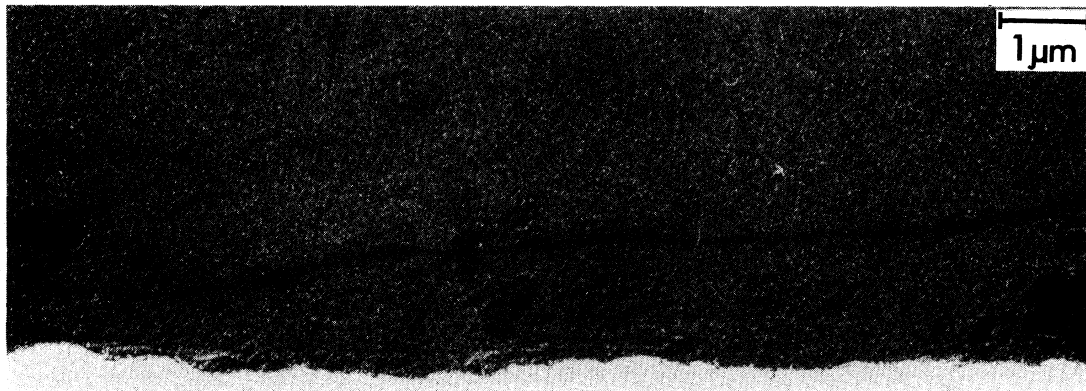
FIG. 4. Permalloy thin film. (a) Lorentz micrograph. (b) Interference micrograph. Magnetic lines of force are directly observed near a cross-tie wall, quite in accordance with the wall structure first predicted by Huber *et al.* (Ref. 14).

formed over a surface enclosed by the two electron trajectories passing through the two points. Applying this principle to thin ferromagnetic film with no stray field, it can be proven that contour lines in the interference image run along in-plane magnetic lines of force inside the film. This is because the phase difference is zero between two points, which lie on the same magnetic line of force. The value of the magnetic flux density can also be determined from the contour map, since a streamtube bordered by two neighboring contour lines contains the constant magnetic flux, h/e . Considering a thin film that is t (Å) thick, with B (Oe), the spacing, x (Å), of the contour lines is given by $h/tBe = 4.1 \times 10^9/tB$. If $t = 1000$ (Å) and $B = 10\,000$ (Oe), then $x = 410$ (Å).

An interference image, and a Lorentz micrograph of a permalloy thin film (Ni 80 at. %—Fe 20 at. %) are shown in Fig. 4. The specimen was prepared by vacuum evaporation and the thickness is approximately 400 Å. In the interference image [Fig. 4(b)], in-plane magnetic lines of force near a cross-tie wall are directly observed as contour lines, quite in accordance with the domain wall structure predicted by

Huber, Smith, and Goodenough.¹⁴ The main 180° wall is made up of Néel- and Bloch-wall sections of opposite polarity, in order to decrease the magnetostatic energy. In a Lorentz micrograph, contrast arises only at the region where the magnetization direction changes abruptly. Hence the main wall and the cross ties, where contour lines change their courses, are observed. In this example, even a smoothly distributed magnetic field can be observed at a glance by interference microscopy, though it is impossible to do so with Lorentz microscopy. An extreme case, where a magnetic field in a free space originated from a specimen edge, could actually be observed in Fig. 4(b). That is, magnetic lines of force are observed as the coarse fringes at the bottom of the figure, which will be more clearly observed in the following two interference images. Magnetic flux density anywhere in the image can be quantitatively determined from contour line spacings, as has been stated.

Speaking precisely, desired conditions do not hold near the centers of the concentric contour lines (Bloch points), where the spin stands up perpendicularly to the film plane. However, Lorentz forces that



(a) Lorentz micrograph

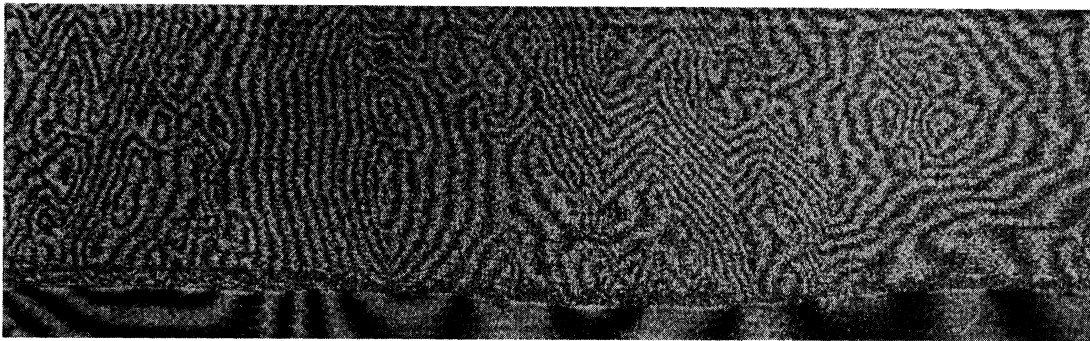


(b) Interference micrograph

FIG. 5. Permalloy thin film. (a) Lorentz micrograph. (b) Interference micrograph. Interference micrograph near a 180° Néel wall indicates how magnetic lines of force change their directions across the wall.



(a) Lorentz micrograph



(b) Interference micrograph

FIG. 6. Nickel thin film. (a) Lorentz micrograph. (b) Interference micrograph. In interference micrograph, circular magnetization is observed, which is barely possible by Lorentz microscopy.

an incident electron beam experiences, both before and after the film, are equal in value and opposite in direction. Therefore, the net effect of the stray field on the electron beam is considered to be small, because of cancellation.

An example of a Néel wall is shown in Fig. 5. The specimen used is a permalloy thin film. Contour lines in Fig. 5(b) show that in-plane magnetic lines of force slowly change their directions across the Néel wall, until they face in the opposite direction. Contour lines do not always coincide with magnetization distribution since magnetization is not divergence-free near a Néel wall and magnetic charge gives rise to a demagnetizing field. Deviation of magnetization from contour lines depends on the amount of demagnetizing field, which is mainly determined by such dimensions as film thickness and wall width. In the present experiment, the deviation is not expected to be large because the film thickness is less than 500 Å.

Another specimen used is a polycrystalline nickel film (Fig. 6). It has a more complex domain wall structure, and consequently it is barely possible to determine fine details of the magnetization by Lorentz microscopy. On the contrary, it is much

easier to interpret the magnetization distribution in the film by interference microscopy. In this specimen, a lot of localized circularly closed magnetic domains are observed.

IV. SUMMARY AND DISCUSSION

Electron holography was developed for investigating the magnetic domain structure of ferromagnetic materials. The technique has been used to investigate magnetization distributions near various kinds of walls, such as the cross-tie wall and Néel wall observed in the present experiment. In-plane magnetic lines of force can be directly seen as contour lines in the interference images. The magnetic lines of force near a cross-tie wall was actually observed confirming the previous prediction. A complex magnetic domain structure, with a magnetization distribution hardly determinable by Lorentz microscopy, can be easily observed by interference microscopy.

Holographic interference microscopy has the following distinctive features when compared with Lorentz microscopy.

(1) Interference micrographs are intuitively interpreted, since the contour lines overlapping electron

microscopic images are magnetic lines of force themselves.

(2) Images need not be defocused, and consequently fine image details of the specimen can be related to its micromagnetic structures.

(3) The averaged magnetic flux density in a specimen can be determined to an absolute value, if the specimen thickness is known. With Lorentz microscopy, however, only a change in it can be detected. An electron hologram contains all the information about the intensity and phase of an electron beam transmitted through a specimen. Lorentz micrographs can even be reconstructed from an electron hologram.

Measurement sensitivity is limited by the electron phase shift of a wavelength, which corresponds to the magnetic flux, h/e . This is also the case with Lorentz microscopy.¹⁵ However, phase-difference amplification¹⁶ can be used in interference microscopy, to ideally reduce the limit down to the magnetic flux $h/14e$. With such a sensitive measurement, careful attention has to be paid to experimental conditions, that may lead to an error.

Errors in measurement result mainly from four factors: (1) nonuniformity of specimen thickness, (2) stray magnetic or electrostatic fields outside a specimen, which may affect the reference beam as well as the object beam itself, (3) distortion of an electron hologram, caused by the magnifying electron lenses, and (4) errors in the optical reconstruction system, especially in a Mach-Zehnder interferometer.

The effect of specimen thickness variation can be removed, at least in principle, by utilizing the different behavior of Lorentz and electrostatic forces through time reversal. An experiment to confirm the applicability of this principle is now in progress.

The effect to stray magnetic fields, originating from a specimen edge on a reference electron beam, can

be estimated from an interference image that is formed where the reference beam in question is regarded as an object.

Progress in electron holography has been made with the development of a new coherent electron source which produces a total of 3000 interference fringes. The quality of holographically reconstructed images has been improved to the extent where they are comparable with electron microscopic images. However, for practical electron holography application, present field-emission electron beams do not have sufficient spatial coherence. A more coherent source is desired to be developed. There is also room for further improvement of beam coherence, even with present field-emission sources that use tungsten tips.

The development of a coherent electron source will open up a new field in coherent electron optics including electron holography, and the latest optical image-processing techniques will become available to electron microscopy.

ACKNOWLEDGMENTS

We would like to express our sincere thanks to Dr. T. Doi at the Central Research Lab., Hitachi Ltd. for promoting the present research and giving us his encouragement. We are indebted to Professor S. Chikazumi at Tokyo University, and Dr. H. Kawakatsu and Dr. S. Tsukahara at the Electrotechnical Laboratory Headquarters, for their valuable discussion on the interpretation of holographic interference microscopy. We also most gratefully acknowledge the valuable advice and stimulation given by Dr. H. Okano, Dr. M. Kudo, Dr. T. Komoda, Dr. Y. Sugita, Dr. F. Nagata, Dr. S. Nomura, Dr. S. Takayama, Dr. R. Suzuki, and Dr. T. Okuwaki at the Central Research Lab., Hitachi Ltd.

¹M. S. Cohen, *J. Appl. Phys.* **38**, 4966 (1967).

²A. Fukuhara, K. Shinagawa, A. Tonomura, and H. Fujiwara (unpublished).

³D. Gabor, *Proc. R. Soc. London Ser. A* **197**, 454 (1949).

⁴D. Gabor, *Proc. Phys. Soc. London, Ser. B* **64**, 449 (1951).

⁵A. Tonomura, *Jpn. J. Appl. Phys.* **11**, 493 (1972).

⁶G. Pozzi and G. F. Missiroli, *J. Microsc. (Paris)* **18**, 103 (1973).

⁷B. Lau and G. Pozzi, *Optik (Stuttgart)* **51**, 287 (1978).

⁸H. Wahl and B. Lau, *Optik (Stuttgart)* **54**, 27 (1979).

⁹A. Tonomura, T. Matsuda, J. Endo, H. Todokoro, and T. Komoda, *J. Electron Microsc.* **28**, 1 (1979).

¹⁰A. Tonomura, T. Matsuda, J. Endo, T. Ariei, and K. Miha-

ma, *Phys. Rev. Lett.* **44**, 1430 (1980).

¹¹G. Möllenstedt and H. Dücker, *Naturwissenschaften* **42**, 41 (1954).

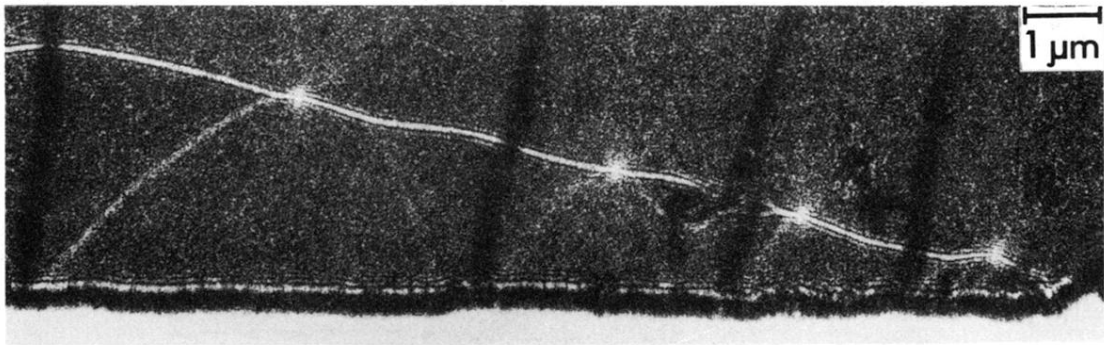
¹²A. Tonomura, J. Endo, and T. Matsuda, *Optik (Stuttgart)* **53**, 143 (1979).

¹³J. Endo, T. Matsuda, and A. Tonomura, *Jpn. J. Appl. Phys.* **18**, 2291 (1979).

¹⁴E. E. Huber, D. O. Smith, and J. B. Goodenough, *J. Appl. Phys.* **29**, 294 (1958).

¹⁵D. Wohlleben, *J. Appl. Phys.* **38**, 3341 (1967).

¹⁶K. Matsumoto and M. Takashima, *J. Opt. Soc. Am.* **60**, 30 (1970).

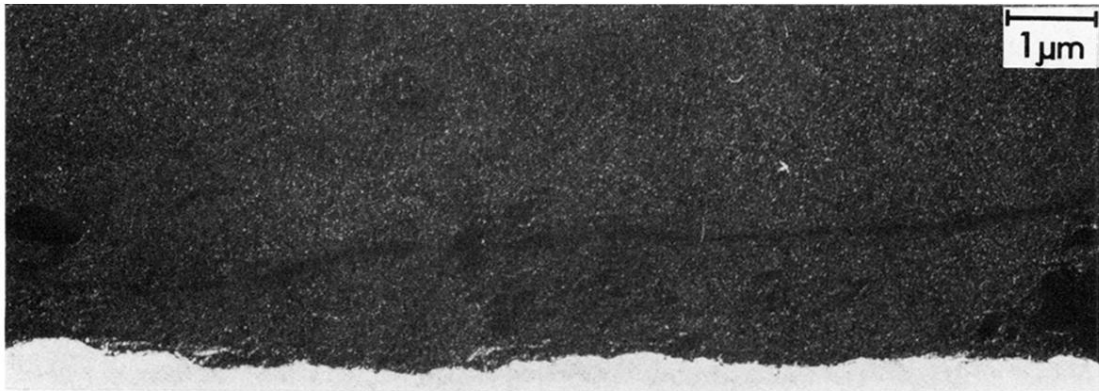


(a) Lorentz micrograph

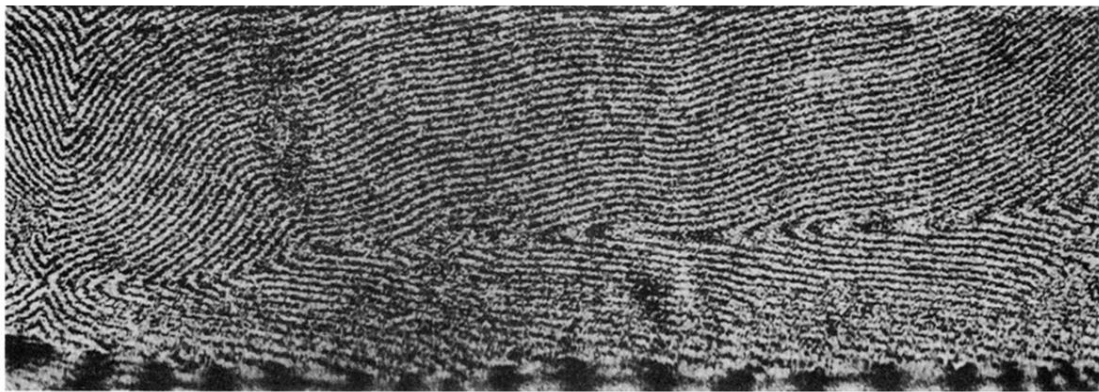


(b) Interference micrograph

FIG. 4. Permalloy thin film. (a) Lorentz micrograph. (b) Interference micrograph. Magnetic lines of force are directly observed near a cross-tie wall, quite in accordance with the wall structure first predicted by Huber *et al.* (Ref. 14).



(a) Lorentz micrograph

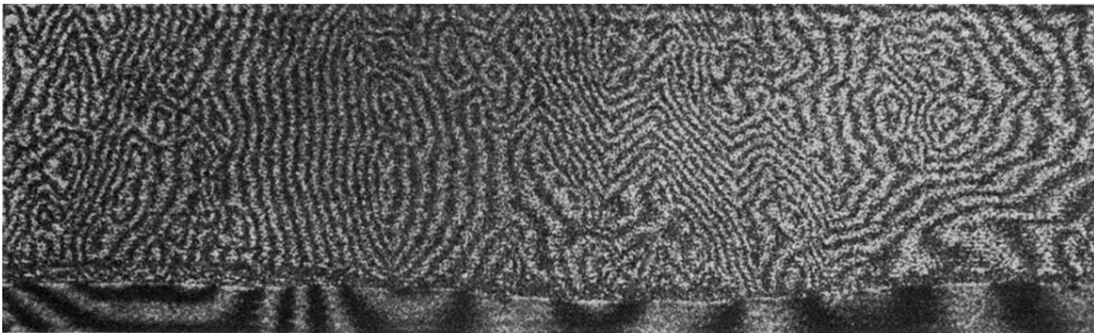


(b) Interference micrograph

FIG. 5. Permalloy thin film. (a) Lorentz micrograph. (b) Interference micrograph. Interference micrograph near a 180° Neel wall indicates how magnetic lines of force change their directions across the wall.



(a) Lorentz micrograph



(b) Interference micrograph

FIG. 6. Nickel thin film. (a) Lorentz micrograph. (b) Interference micrograph. In interference micrograph, circular magnetization is observed, which is barely possible by Lorentz microscopy.